Zero- and infinite-frequency limits of P-wave traveltime parameters in tilted orthorhombic media

Yuriy Ivanov* and Alexey Stovas

Norwegian University of Science and Technology (NTNU)
Department of Petroleum Engineering & Applied Geophysics
E-mail: yuriy.ivanov@ntnu.no

April 25th, 2016
ROSE meeting

NTNU – Trondheim
Norwegian University of Science and Technology

Outline

Background

- Propagation of seismic waves through a layered (and anisotropic) medium is frequency dependent,

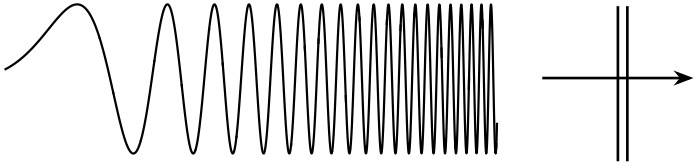

Background

- Propagation of seismic waves through a layered (and anisotropic) medium is frequency dependent,
- P-wave propagation velocity in isotropic layered medium variation between zero- and infinite-frequency limits can reach 15% (Stovas and Ursin, 2007),

Background

- Propagation of seismic waves through a layered (and anisotropic) medium is frequency dependent,
- P-wave propagation velocity in isotropic layered medium variation between zero- and infinite-frequency limits can reach 15% (Stovas and Ursin, 2007),
- Although, we never face zero- or infinite-frequency propagation in reality, it is important to know the values at these limits,

Background

- Propagation of seismic waves through a layered (and anisotropic) medium is frequency dependent,
- P-wave propagation velocity in isotropic layered medium variation between zero- and infinite-frequency limits can reach 15% (Stovas and Ursin, 2007),
- Although, we never face zero- or infinite-frequency propagation in reality, it is important to know the values at these limits,
- In light of increasing application of orthorhombic (ORT) and tilted orthorhombic (TOR) models in industry, it is practically important to consider the two frequency limits in these models,

Background

- Propagation of seismic waves through a layered (and anisotropic) medium is frequency dependent,
- P-wave propagation velocity in isotropic layered medium variation between zero- and infinite-frequency limits can reach 15% (Stovas and Ursin, 2007),
- Although, we never face zero- or infinite-frequency propagation in reality, it is important to know the values at these limits,
- In light of increasing application of orthorhombic (ORT) and tilted orthorhombic (TOR) models in industry, it is practically important to consider the two frequency limits in these models,
- We analyze the traveltime (processing) parameters (and geometrical spreading) of the reflected P-wave in two frequency limits as a function of the symmetry planes tilt in orthorhombic medium.

Goals

- Derive zero- and infinite-frequency limits of the traveltime parameters for reflected waves in layered TOR media,

Goals

- Derive zero- and infinite-frequency limits of the traveltime parameters for reflected waves in layered TOR media,
- Compare the two limits using numerical model,

Goals

- Derive zero- and infinite-frequency limits of the traveltime parameters for reflected waves in layered TOR media,
- Compare the two limits using numerical model,
- Compare the two limits using real data (well log),

Goals

- Derive zero- and infinite-frequency limits of the traveltime parameters for reflected waves in layered TOR media,
- Compare the two limits using numerical model,
- Compare the two limits using real data (well log),
- Analyze the relative geometrical spreading in the frequency limits using numerical model and well log data.

The model

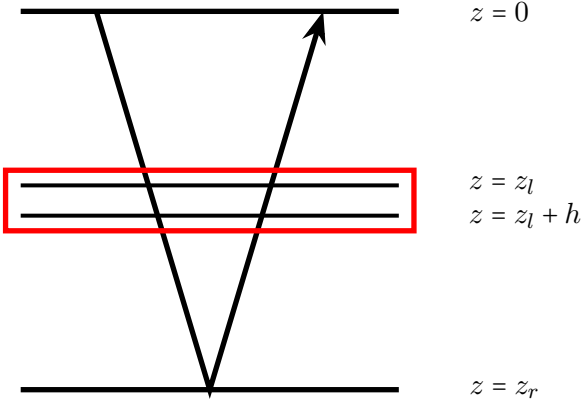

Figure 1: Schematic propagation of a pure reflected wave-mode through a TOR layer.

The model

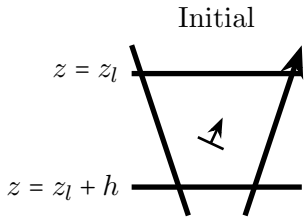

Figure 2: An enlarged version of an area inside the red rectangle in Figure 1. Symbol ↥ schematically indicates the orthorhombic symmetry planes tilt.

The model

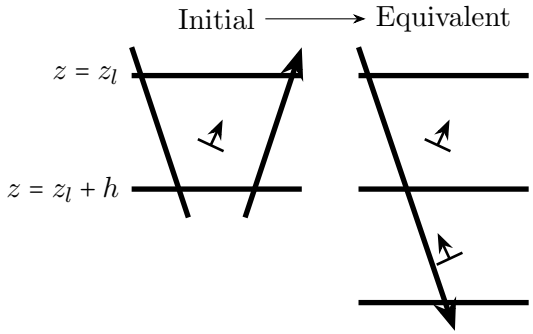

Figure 2: An enlarged version of an area inside the red rectangle in Figure 1. Symbol ↥ schematically indicates the orthorhombic symmetry planes tilt.

The model

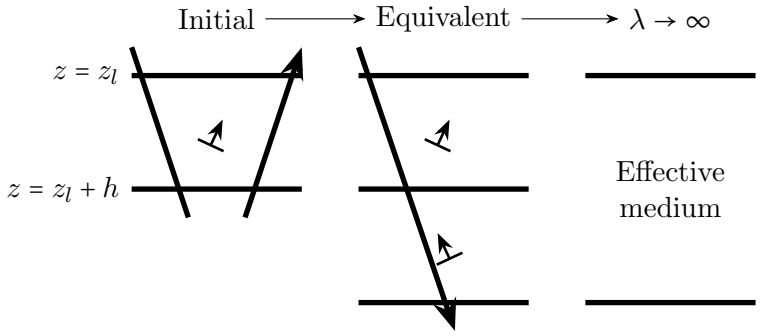

Figure 2: An enlarged version of an area inside the red rectangle in Figure 1. Symbol ↕ schematically indicates the orthorhombic symmetry planes tilt.

The model

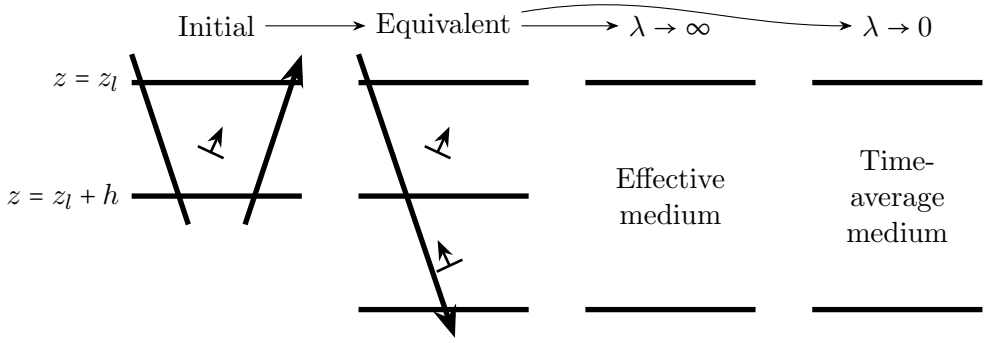

Figure 2: An enlarged version of an area inside the red rectangle in Figure 1. Symbol ↕ schematically indicates the orthorhombic symmetry planes tilt.

Zero-frequency limit, $\lambda \gg h$

Elastic orthorhombic stiffness matrix

$$\mathbf{c}^{\mathrm{ORT}} = \begin{pmatrix} c_{11} & c_{12} & c_{13} & 0 & 0 & 0 \\ & c_{22} & c_{23} & 0 & 0 & 0 \\ & & c_{33} & 0 & 0 & 0 \\ & \mathrm{SYM} & & c_{44} & 0 & 0 \\ & & & & c_{55} & 0 \\ & & & & & c_{66} \end{pmatrix}. \tag{1}$$

Tilted elastic orthorhombic stiffness matrix

$$\mathbf{c}^{\mathrm{TOR}} = \mathbf{R}_\theta \mathbf{c}^{\mathrm{ORT}} \mathbf{R}_\theta^{\mathrm{T}}, \tag{2}$$

where $\mathbf{R}_\theta$ is the Bond transformation matrix, needed to rotate the stiffness matrix in Voigt notation about the x_2-axis at an angle θ.

Euler's angle θ

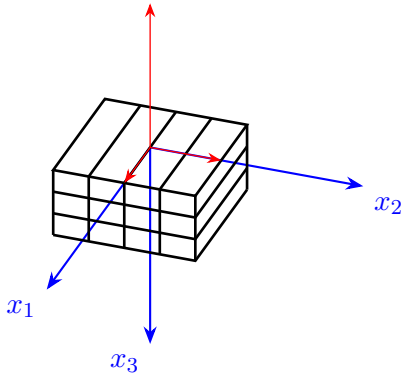

Euler's angle θ

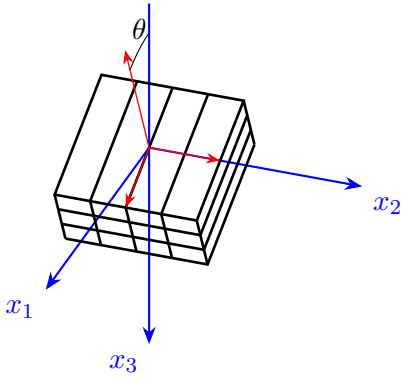

Schoenberg and Muir upscaling

Theory of Schoenberg and Muir (1989) is an extension of the Backus (1962) upscaling to an arbitrary anisotropic media. Using this theory we obtain the effective anisotropic medium for a reflected wave:

$$\tilde{\mathbf{c}} = \left\langle \mathbf{c}^{\mathrm{TOR}}(\theta), \mathbf{c}^{\mathrm{TOR}}(-\theta) \right\rangle, \tag{3}$$

where $\langle ... \rangle$ denotes the upscaling operation. Structure of $\tilde{\mathbf{c}}$ is similar to that of a vertical ORT medium and defined by 10 independent parameters.

Infinite-frequency limit, $\lambda \ll h$

Time (slowness surface) averaging

In order to obtain the traveltime parameters in the infinite-frequency limit (ray approximation), slowness surfaces should be averaged:

$$p_3^{(R)}(\theta) = \frac{p_3^{(D)}(\theta) + p_3^{(U)}(\theta)}{2} \tag{4}$$

where $\mathbf{p} = (p_1, p_2, p_3)^{\mathrm{T}}$ is the slowness vector, $p_3 = p_3(p_1, p_2)$, and R, D, and U in p_3 superscript indicates "reflected", "down"- and "up"-traveling wave.

Time (slowness surface) averaging

In order to obtain the traveltime parameters in the infinite-frequency limit (ray approximation), slowness surfaces should be averaged:

$$p_3^{(R)}(\theta) = \frac{p_3^{(D)}(\theta) + p_3^{(U)}(\theta)}{2} = \frac{p_3(\theta) + p_3(-\theta)}{2}, \tag{4}$$

where $\mathbf{p} = (p_1, p_2, p_3)^{\mathrm{T}}$ is the slowness vector, $p_3 = p_3(p_1, p_2)$, and R, D, and U in p_3 superscript indicates "reflected", "down"- and "up"-traveling wave.

Traveltime parameters

Series for the traveltime squared

Traveltime parameters are related to the coefficients in front of the source-receiver offset horizontal projections in the series for traveltime squared:

$$t^2(x_1, x_2) = \frac{z^2}{V_0^2} + \frac{x_1^2}{V_{n2}^2} + \frac{x_2^2}{V_{n1}^2} - \frac{2\eta_2 x_1^4}{V_{n2}^4 t_0^2} - \frac{2\eta_1 x_2^4}{V_{n1}^4 t_0^2} - \frac{2\eta_{xy} x_1^2 x_2^2}{V_{n2}^2 V_{n1}^2 t_0^2} + ..., \tag{5}$$

Series for the traveltime squared

Traveltime parameters are related to the coefficients in front of the source-receiver offset horizontal projections in the series for traveltime squared:

$$t^2(x_1, x_2) = \frac{z^2}{V_0^2} + \frac{x_1^2}{V_{n2}^2} + \frac{x_2^2}{V_{n1}^2} - \frac{2\eta_2 x_1^4}{V_{n2}^4 t_0^2} - \frac{2\eta_1 x_2^4}{V_{n1}^4 t_0^2} - \frac{2\eta_{xy} x_1^2 x_2^2}{V_{n2}^2 V_{n1}^2 t_0^2} + ..., \tag{5}$$

where V_0 is the velocity along the vertical, z - thickness of the layer, V_{n2}, η_2 and V_{n1}, η_1 are (P-wave) normal move-out velocities and anellipticity parameters in $[x_1, x_3]$ and $[x_2, x_3]$ planes, respectively (Tsvankin, 1997), η_{xy} is the cross-term anellipticity (Stovas, 2015).

Traveltime parameters

Traveltime parameters are obtained from the offset-traveltime parametric equations

$$\begin{cases} x_1(p_1, p_2) = -z\dfrac{\partial p_3}{\partial p_1}, \\ x_2(p_1, p_2) = -z\dfrac{\partial p_3}{\partial p_2}, \\ t(p_1, p_2) = x_1 p_1 + x_2 p_2 + z p_3. \end{cases} \tag{6}$$

Frequency limits comparison

Weak anisotropy expressions, first order

In weak anisotropy approximation, the expressions are identical up to the first order in anisotropy parameters:

$$
\begin{aligned}
V_{P0}^{LF} &= V_{P0}^{HF} = V_{\mathrm{P}0}\left(1+\epsilon_2\sin^4\theta+\delta_2\sin^2\theta\cos^2\theta\right),\\
V_{n1}^{LF} &= V_{n1}^{HF} = V_{\mathrm{P}0}\left[1+\epsilon_2(1+\cos^2\theta)\sin^2\theta+\delta_1\cos^2\theta-\delta_2\sin^2\theta\cos^2\theta+\delta_3\sin^2\theta\right],\\
V_{n2}^{LF} &= V_{n2}^{HF} = V_{\mathrm{P}0}\left[1+\epsilon_2(7\cos^2\theta-1)\sin^2\theta+\delta_2(1-7\sin^2\theta\cos^2\theta)\right],\\
\eta_1^{LF} &= \eta_1^{HF} = \epsilon_1-\epsilon_2(1+\cos^2\theta)\sin^2\theta-\delta_1\cos^2\theta+\delta_2\sin^2\theta\cos^2\theta-\delta_3\sin^2\theta,\\
\eta_2^{LF} &= \eta_2^{HF} = (\epsilon_2-\delta_2)\cos 4\theta,\\
\eta_{xy}^{LF} &= \eta_{xy}^{HF} = (\epsilon_2-\delta_1+\delta_3)\cos 2\theta+(\epsilon_2-\delta_2)\cos 4\theta,
\end{aligned}
\tag{7}
$$

where superscripts LF and HF correspond to zero- and infinite-frequency limits, respectively. Tsvankin (1997) notation is used.

Weak anisotropy expressions, second order

The relation between vertical P-wave velocity ($\sqrt{c_{33}}$) in frequency limits up to the second order in anisotropy parameters:

$$\frac{V_{P0}^{HF}}{V_{P0}^{LF}} = 1 + \frac{\sin^2 2\theta}{2g(1-g)}\left(\epsilon_2^2 \sin^4\theta + \delta_2^2 \frac{\cos^2 2\theta}{4} + \epsilon_2\delta_2 \sin^2\theta \cos 2\theta\right) + ..., \tag{8}$$

where $g \equiv V_{S0}^2/V_{P0}^2$.

Contribution from the individual terms

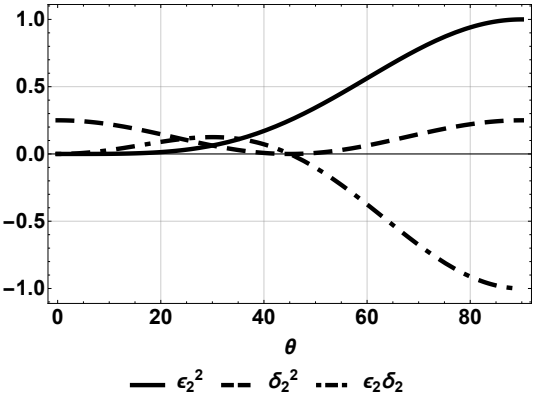

Weak anisotropy expressions, second order

S1- ($\sqrt{c_{55}}$) and S2- ($\sqrt{c_{44}}$) waves:

$$\frac{V_{S10}^{HF}}{V_{S10}^{LF}} = 1 - \frac{\sin^2 2\theta}{2g(1-g)}\left(\epsilon_2^2 \sin^4\theta + \delta_2^2 \frac{\cos^2 2\theta}{4} + \epsilon_2\delta_2 \sin^2\theta \cos 2\theta\right) + ...,$$
$$\frac{V_{S20}^{HF}}{V_{S20}^{LF}} = 1. \tag{9}$$

Correspondence between the vertical velocities

$$
\begin{aligned}
V_{P0}^{HF} &\geq V_{P0}^{LF}, \\
V_{S10}^{HF} &\leq V_{S10}^{LF}, \\
V_{S20}^{HF} &= V_{S20}^{LF}.
\end{aligned}
\tag{10}
$$

Single TOR layer

Layer parameters:

V_{P0} =4 km/s, ϵ_2 = 0.25 δ_2 = 0.15, γ_2 = 0.1, δ_3 = 0.15,
V_{S0} =2 km/s, ϵ_1 = 0.15 δ_1 = 0.05, γ_1 = 0.15.

Single TOR layer

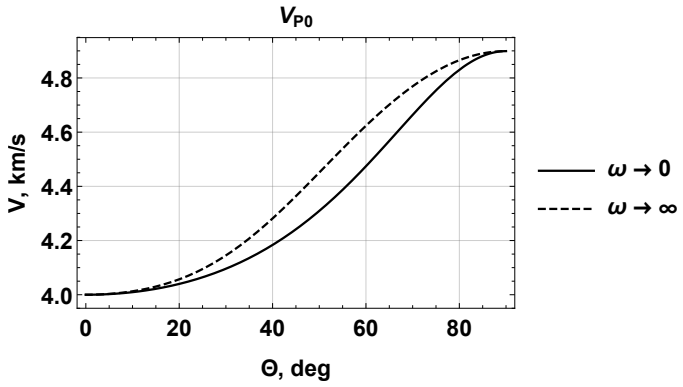

Single TOR layer

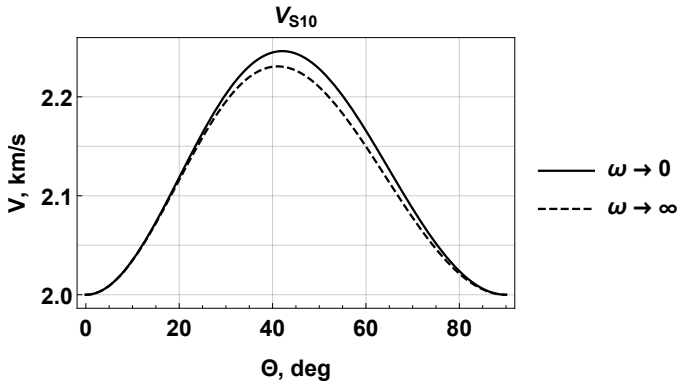

Single TOR layer

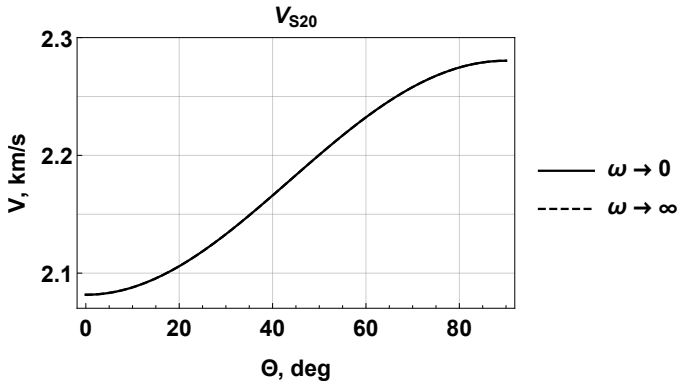

Single TOR layer

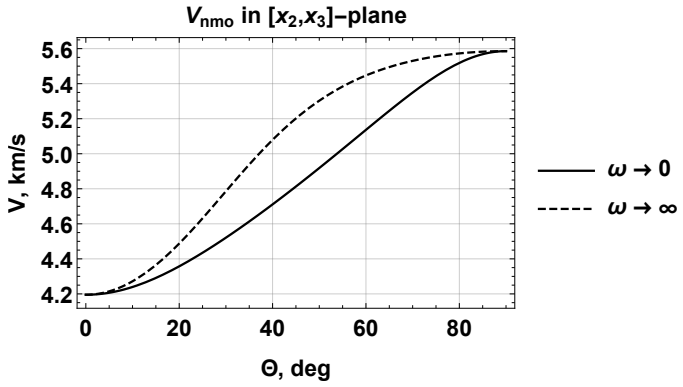

Single TOR layer

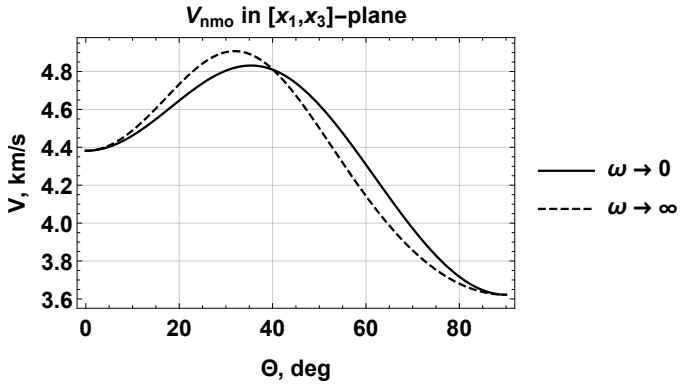

Single TOR layer

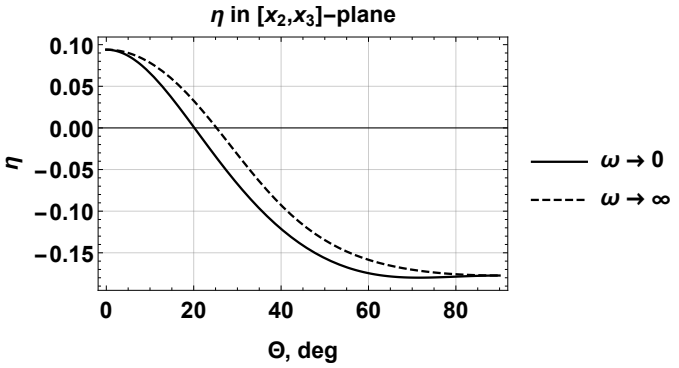

Single TOR layer

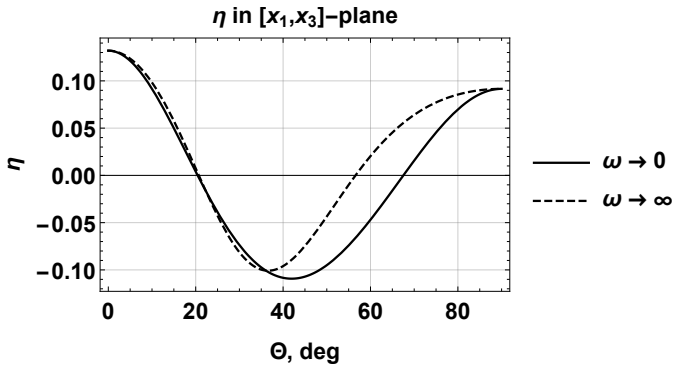

Single TOR layer

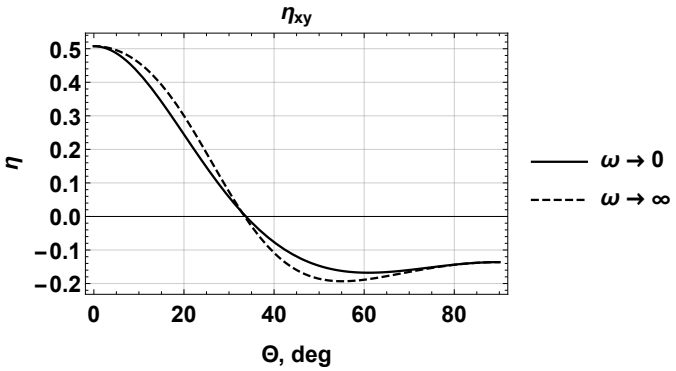

Heterogeneous TOR medium: real well log data

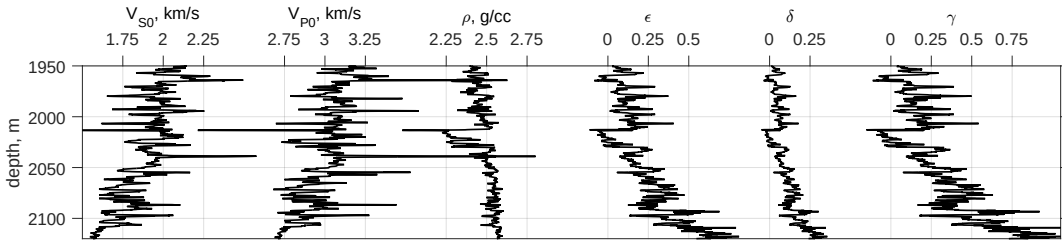

Courtesy of Statoil ASA

We use the theory of Schoenberg and Helbig (1997) to include penny-shaped gas-filled cracks, $\delta_N = 0.2$, $\delta_T = 0.5$ (Bakulin et al., 2000), in VTI stiffness matrix along the $[x_2, x_3]$ plane in order to make the medium orthorhombic.

Well log data - uniform tilt

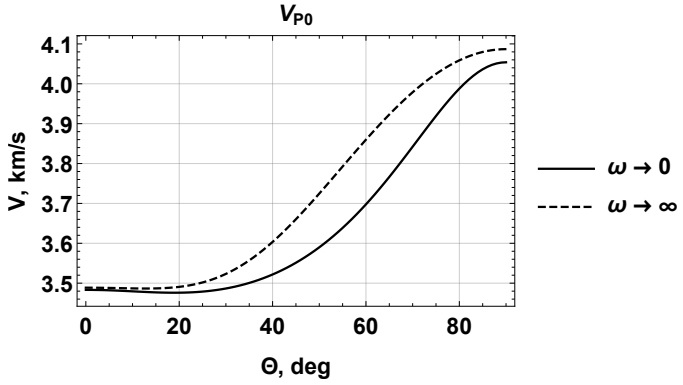

Well log data - uniform tilt

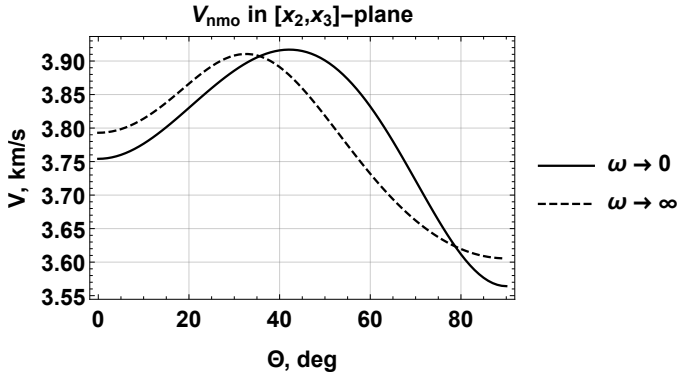

Well log data - uniform tilt

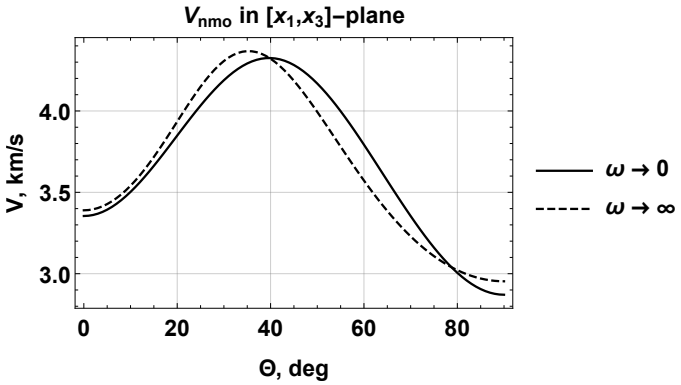

Well log data - uniform tilt

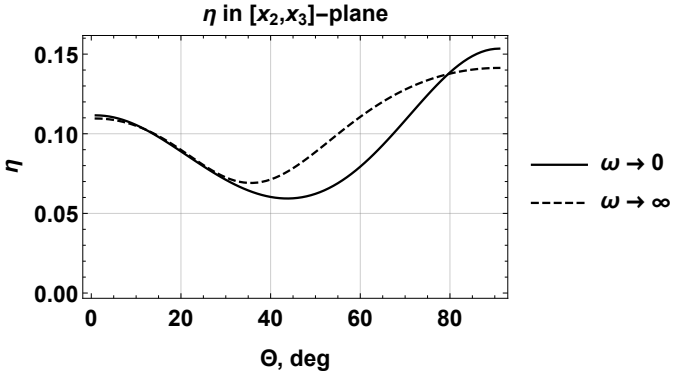

Well log data - uniform tilt

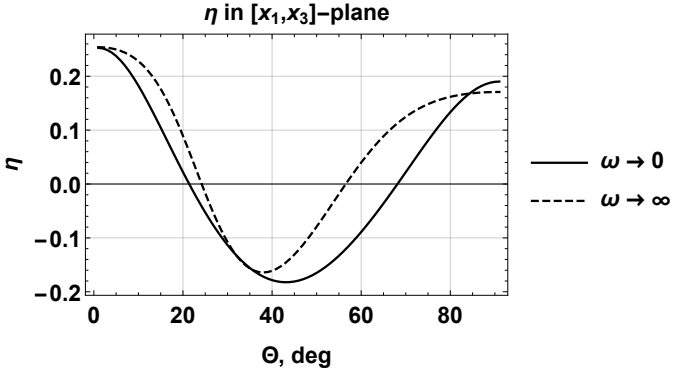

Well log data - uniform tilt

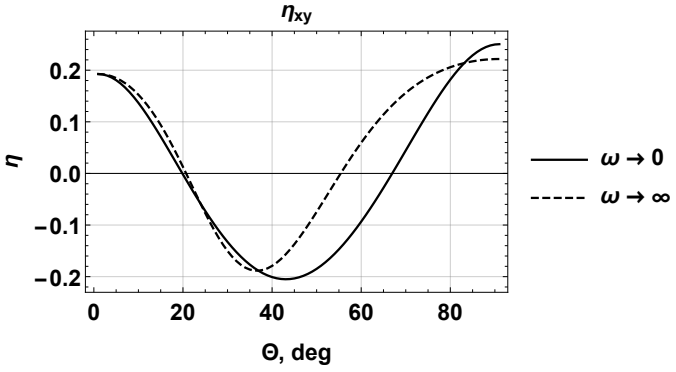

Relative geometrical spreading

Relative geometrical spreading $\mathcal{L}$

$$A \propto \frac{1}{\mathcal{L}(x_1, x_2)} \tag{11}$$

where A is the wave amplitude, x_1 and x_2 are the source-receiver offset projections.

Relative geometrical spreading $\mathcal{L}$

$$A \propto \frac{1}{\mathcal{L}(x_1, x_2)} \propto \det \mathbf{M} = -\begin{pmatrix} \frac{\partial^2 T(x_1,x_2)}{\partial x_1^2} & \frac{\partial^2 T(x_1,x_2)}{\partial x_1 \partial x_2} \\ \frac{\partial^2 T(x_1,x_2)}{\partial x_2 \partial x_1} & \frac{\partial^2 T(x_1,x_2)}{\partial x_2^2} \end{pmatrix}, \tag{11}$$

where A is the wave amplitude, x_1 and x_2 are the source-receiver offset projections.

Relative geometrical spreading $\mathcal{L}$

$$A \propto \frac{1}{\mathcal{L}(x_1, x_2)} \propto \det \mathbf{M} = -\begin{pmatrix} \frac{\partial^2 T(x_1,x_2)}{\partial x_1^2} & \frac{\partial^2 T(x_1,x_2)}{\partial x_1 \partial x_2} \\ \frac{\partial^2 T(x_1,x_2)}{\partial x_2 \partial x_1} & \frac{\partial^2 T(x_1,x_2)}{\partial x_2^2} \end{pmatrix}, \tag{11}$$

where A is the wave amplitude, x_1 and x_2 are the source-receiver offset projections.
Convenient to display the normalized quantity:

$$\frac{\mathcal{L}^{-1}}{\mathcal{L}^{-1}_{\text{ISO}}},$$

where $\mathcal{L}_{\text{ISO}}$ is calculated in isotropic medium with the velocity equal to the vertical velocity in the initial orthorhombic medium.

Single TOR layer

Layer parameters:

V_{P0} =4 km/s, ϵ_2 = 0.25 δ_2 = 0.15, γ_2 = 0.1, δ_3 = 0.15,
V_{S0} =2 km/s, ϵ_1 = 0.15 δ_1 = 0.05, γ_1 = 0.15.

Tilt $\theta = 0$

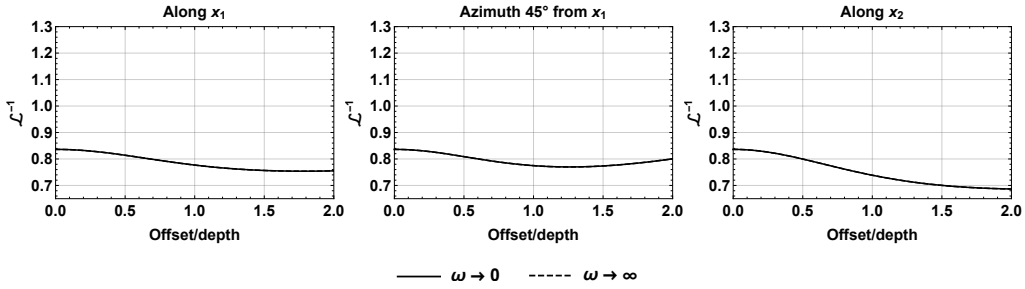
Along x_1
Azimuth 45° from x_1
Along x_2
$\mathcal{L}^{-1}$
1.3
1.2
1.1
1.0
0.9
0.8
0.7
0.0
0.5
1.0
1.5
2.0
Offset/depth
$\omega \to 0$
$\omega \to \infty$

Tilt $\theta = 30°$

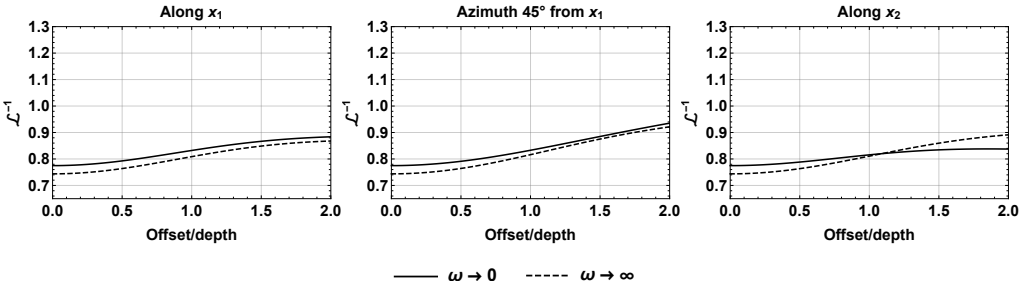

Tilt $\theta = 60°$

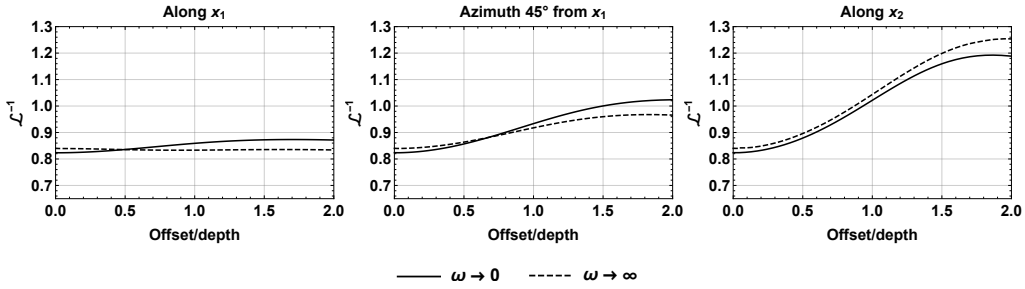

Heterogeneous TOR medium: real well log data

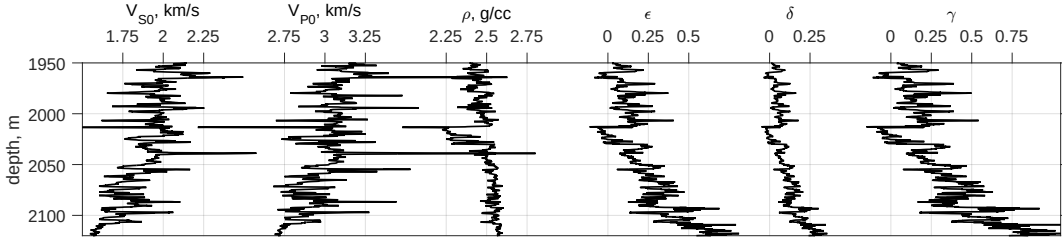

Courtesy of Statoil ASA

Tilt $\theta = 0$

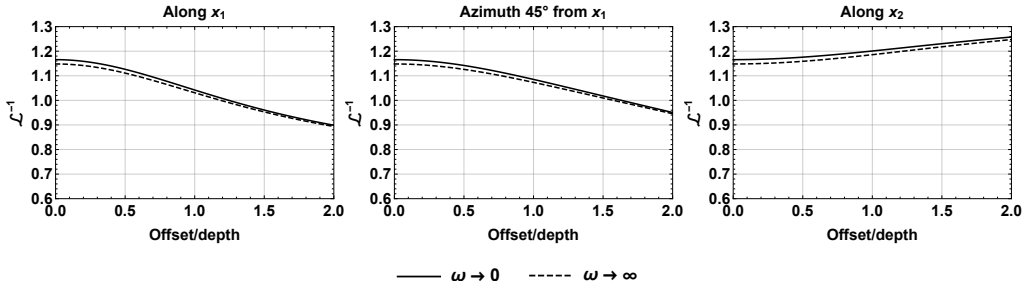
Along x_1
Azimuth 45° from x_1
Along x_2
$\mathcal{L}^{-1}$
Offset/depth
$\omega \to 0$
$\omega \to \infty$

Tilt $\theta = 30°$

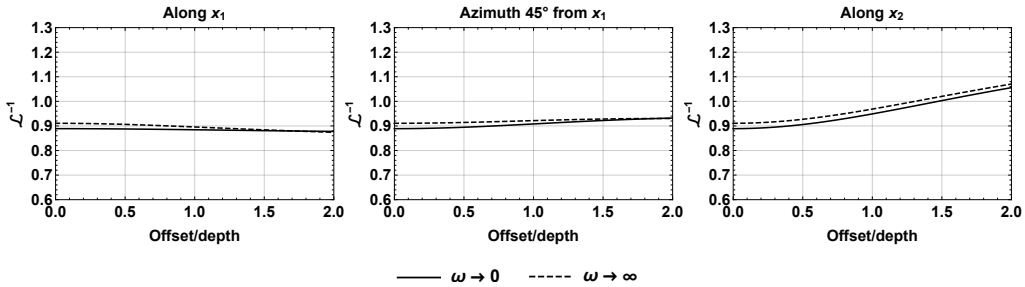

Tilt $\theta = 60°$

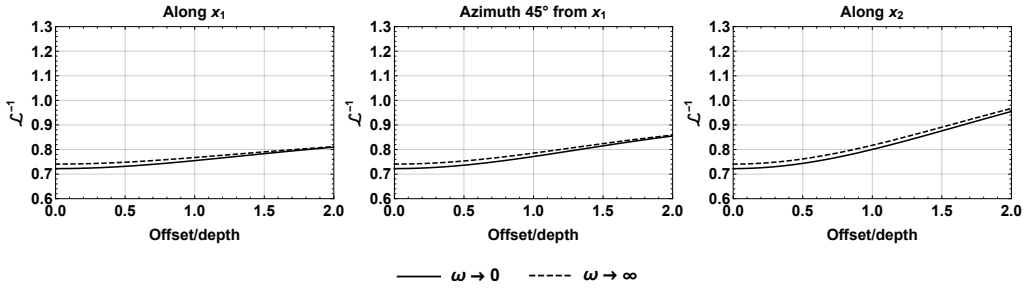

Conclusions

- Traveltime parameters of the reflected P-wave in tilted orthorhombic medium in zero- and infinite-frequency limits are analyzed,

Conclusions

- Traveltime parameters of the reflected P-wave in tilted orthorhombic medium in zero- and infinite-frequency limits are analyzed,
- Weak-anisotropy approximation for the P-wave traveltime parameters are derived and it is shown that they are equal in the frequency limits,

Conclusions

- Traveltime parameters of the reflected P-wave in tilted orthorhombic medium in zero- and infinite-frequency limits are analyzed,
- Weak-anisotropy approximation for the P-wave traveltime parameters are derived and it is shown that they are equal in the frequency limits,
- Algebraically and using a well log data we demonstrate that the vertical P-wave velocity is higher in the infinite-frequency limit than in the zero-frequency,

Conclusions

- Traveltime parameters of the reflected P-wave in tilted orthorhombic medium in zero- and infinite-frequency limits are analyzed,
- Weak-anisotropy approximation for the P-wave traveltime parameters are derived and it is shown that they are equal in the frequency limits,
- Algebraically and using a well log data we demonstrate that the vertical P-wave velocity is higher in the infinite-frequency limit than in the zero-frequency,
- The vertical S1-wave velocity is lower in the infinite-frequency limit than in the zero-frequency, the S2-wave velocity is equal in both frequency limits,

Conclusions

- Traveltime parameters of the reflected P-wave in tilted orthorhombic medium in zero- and infinite-frequency limits are analyzed,
- Weak-anisotropy approximation for the P-wave traveltime parameters are derived and it is shown that they are equal in the frequency limits,
- Algebraically and using a well log data we demonstrate that the vertical P-wave velocity is higher in the infinite-frequency limit than in the zero-frequency,
- The vertical S1-wave velocity is lower in the infinite-frequency limit than in the zero-frequency, the S2-wave velocity is equal in both frequency limits,
- Correspondence of other parameters (incl. geometrical spreading) in the frequency limits is not simple, however, the difference in effective parameters between two limits can be significant, and it should be analyzed prior to averaging of log data.

Discussion and future work

- Equivalence of the weak-anisotropy expressions in two frequency limits suggests that we can use the isotropic model for the dispersion analysis if anisotropy is indeed weak (!),

Discussion and future work

- Equivalence of the weak-anisotropy expressions in two frequency limits suggests that we can use the isotropic model for the dispersion analysis if anisotropy is indeed weak (!),
- The approach can be extended to more realistic TOR model with the symmetry planes rotated about an arbitrary vector.

Acknowledgments

Authors are thankful to the ROSE project for the financial support. I thank Ivan Karpov for fruitful discussions.

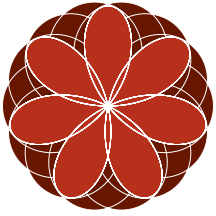

Thanks for your attention.

References

Backus, G. E., 1962, Long-wave elastic anisotropy produced by horizontal layering: Journal of Geophysical Research, **67**, 4427–4440.

Bakulin, A., V. Grechka, and I. Tsvankin, 2000, Estimation of fracture parameters from reflection seismic data; Part I, HTI model due to a single fracture set: Geophysics, **65**, 1788–1802.

Schoenberg, M., and K. Helbig, 1997, Orthorhombic media: Modeling elastic wave behavior in a vertically fractured earth: Geophysics, **62**, 1954–1974.

Schoenberg, M., and F. Muir, 1989, A calculus for finely layered anisotropic media: Geophysics, **54**, 581–589.

Stovas, A., 2015, Azimuthally dependent kinematic properties of orthorhombic media: Geophysics, **80**, C107–C122.

Stovas, A., and B. Ursin, 2007, Equivalent time-average and effective medium for periodic layers: Geophysical Prospecting, **55**, 871–882.

Tsvankin, I., 1997, Anisotropic parameters and P-wave velocity for orthorhombic media: Geophysics, **62**, 1292–1309.

Schoenberg and Muir method

$$\bar{\mathbf{C}}_{\mathrm{NN}} = \left\langle \mathbf{C}_{\mathrm{NN}}^{-1} \right\rangle^{-1},$$
$$\bar{\mathbf{C}}_{\mathrm{TN}} = \left\langle \mathbf{C}_{\mathrm{TN}} \mathbf{C}_{\mathrm{NN}}^{-1} \right\rangle \bar{\mathbf{C}}_{\mathrm{NN}},$$
$$\bar{\mathbf{C}}_{\mathrm{TT}} = \left\langle \mathbf{C}_{\mathrm{TT}} \right\rangle - \left\langle \mathbf{C}_{\mathrm{TN}} \mathbf{C}_{\mathrm{NN}}^{-1} \mathbf{C}_{\mathrm{NT}} \right\rangle + \left\langle \mathbf{C}_{\mathrm{TN}} \mathbf{C}_{\mathrm{NN}}^{-1} \right\rangle \bar{\mathbf{C}}_{\mathrm{NN}} \left\langle \mathbf{C}_{\mathrm{NN}}^{-1} \mathbf{C}_{\mathrm{NT}} \right\rangle,$$

with

$$\mathbf{C}_{\mathrm{NN}}^{i} = \begin{pmatrix} C_{33}^{i} & C_{34}^{i} & C_{35}^{i} \\ C_{34}^{i} & C_{44}^{i} & C_{45}^{i} \\ C_{35}^{i} & C_{45}^{i} & C_{55}^{i} \end{pmatrix}, \quad \mathbf{C}_{\mathrm{TN}}^{i} = \begin{pmatrix} C_{13}^{i} & C_{14}^{i} & C_{15}^{i} \\ C_{23}^{i} & C_{24}^{i} & C_{25}^{i} \\ C_{36}^{i} & C_{46}^{i} & C_{56}^{i} \end{pmatrix}, \quad \mathbf{C}_{\mathrm{TT}}^{i} = \begin{pmatrix} C_{11}^{i} & C_{12}^{i} & C_{16}^{i} \\ C_{12}^{i} & C_{22}^{i} & C_{26}^{i} \\ C_{16}^{i} & C_{26}^{i} & C_{66}^{i} \end{pmatrix}.$$

Vertically fractured VTI

$$\mathbf{C}^{\mathrm{VFVTI}} = \begin{pmatrix} C_{11b}(1-\delta_N) & C_{12b}(1-\delta_N) & C_{13b}(1-\delta_N) & 0 & 0 & 0 \\ & C_{11b}-\delta_N\frac{C_{12b}^2}{C_{11b}} & C_{13b}\left(1-\delta_N\frac{C_{12b}}{C_{11b}}\right) & 0 & 0 & 0 \\ & & C_{33b}-\delta_N\frac{C_{13b}^2}{C_{11b}} & 0 & 0 & 0 \\ & \mathrm{SYM} & & C_{44b} & 0 & 0 \\ & & & & C_{44b}(1-\delta_V) & 0 \\ & & & & & C_{66b}(1-\delta_H) \end{pmatrix},$$

where

$$0 \le \delta_N \equiv \frac{Z_N C_{11b}}{1+Z_N C_{11b}} \le 1, \qquad 0 \le \delta_V \equiv \frac{Z_V C_{44b}}{1+Z_V C_{44b}} \le 1, \qquad 0 \le \delta_H \equiv \frac{Z_H C_{66b}}{1+Z_H C_{66b}} \le 1.$$